Investigation of the Relationship Between the Yucatan Channel Transport and the Loop Current Area in a Multidecadal Numerical Simulation

AUTHORS

Robert Nedbor-Gross
Dmitry S. Dukhovskoy
Mark A. Bourassa
Steven L. Morey
Eric P. Chassignet
Center for Ocean-Atmospheric
Prediction Studies,
The Florida State University

Introduction

The loop current (LC) is a part of the North Atlantic western boundary current system that enters the Gulf of Mexico (GoM) through the Yucatan Channel (YC), loops in a clockwise manner, and exits through the Florida Straits (FLS). The location and growth rate of the LC are highly variable on annual to interannual time scales. The LC goes through several phases during its life cycle. During a retracted phase, the LC does not extend far into the GoM and is considered to be stable in that its configuration is not likely to change rapidly through the development of large-scale meanders or the shedding of large eddies. When extended far north, the LC is in a configuration that is favorable for the formation of LC eddies (LCEs), which are large anticyclonic rings that break off from the LC, referred to as a shedding event, and propagate westward through the GoM. As shown in previous studies (Hurlburt & Thompson,

ABSTRACT

A hypothesis by Maul (1977), stating the rate of change of loop current (LC) volume is related to deep Yucatan Channel (YC) transport, is tested with a continuous 54-year simulation of the Gulf of Mexico (GoM) using a regional 1/25° resolution Hybrid Coordinate Ocean Model (HYCOM) configuration. The hypothesis states that the imbalance of transport between the upper YC and the Florida Straits controls the rate of change of the LC volume and that the imbalance is compensated by transport through the deep YC. Bunge et al. (2002) found a strong relationship between the deep YC transport and the LC area using 7.5 months of data from a mooring array in the YC, but the observational record length was relatively short compared to the time scale of LC variability. The 54-year HYCOM simulation provides a much longer and spatially complete data set to study the LC variability. Results show that the time evolution of the LC between two shedding events can be viewed as a combination of relatively high-frequency fluctuations superimposed on a low-frequency trend. The high-frequency variability of the LC area time derivative and the deep YC transport are related. The low-frequency variability is examined by comparing the LC area time series with time-integrated transport in the deep YC, and statistically similar trends are identified, supporting the Maul (1977) theory.
Keywords: Loop Current, Gulf of Mexico, HYCOM, Yucatan Channel

1980; Sturges, 1994), this extended LC is an "unstable configuration," a configuration into which it must evolve in order to shed an LCE. Shedding events, like the LC, are variable in time and difficult to predict. Understanding the mechanisms that govern the LC and LCEs is important for predicting their variability.

Understanding of the LC and LCE processes is important for several practical reasons. The strong currents associated with the LCEs (which may approach 3 m/s) affect oil and gas production facilities in the GoM. Their associated surface (as well as subsur-face) currents may transport contaminants far from their release location, as was the case with the 2010 oil spill from the BP Macondo well blowout. Also, LCEs and the LC can generate very strong deep currents in the regions of oil and gas development (Dukhovskoy et al., 2009; Morey & Dukhovskoy, 2013), and accurate predictions of the LC and LCEs are useful for operational planning and engineering of platforms and pipelines in these regions. In addition, the deep, warm water associated with LCEs and the LC can provide a source of energy for hurricane intensification, as may have been the case in

2005 when Hurricane Katrina intensified from category 3 to category 5 as it moved over the LC (Gierach et al., 2009).

Whether the LC evolution can be predicted is an open question. From altimeter data, Leben (2005) found a robust linear relationship between the northern retreat latitude after the LC sheds an eddy and consequent eddy shedding periods. Lugo-Fernandez (2007) suggested that the LC could be viewed as nonchaotic dynamical system with limited predictability. Nevertheless, LC behavior is irregular, and its prediction is still challenging especially in practical applications, which often require prediction for specific locations (i.e., oil rigs). A better knowledge of the mechanisms controlling the LC behavior may provide additional insight into limitations and possibilities of LC predictions.

This study investigates the relationship between deep YC transport and LC volume changes. Maul (1977) first suggested that the LC grows because of a mass imbalance between the transport into the GoM through the upper YC and the transport out through the FLS. The LC grows when the mass entering the upper YC exceeds the mass exiting the FLS. Since the rate of change of the GoM's volume is negligible, the mass imbalance created must be compensated for somewhere else. Maul (1977) suggested that the imbalance is compensated by deep flows in the lower YC. Thus, the deep YC transport should be related to the rate of change of the LC volume. This is possible because the depth of the YC is about twice that of the FLS. Maul et al. (1985) examined this idea using a current meter placed near the bottom and in the middle of the YC. They collected 3 years of data and found no significant rela-

tionship between deep flows in the YC and the rate of change of LC size inferred from the area obtained via satellite measurements. Maul and Vukovich (1993) examined volume transport through the FLS and also did not find a significant relation to the LC area rate of change.

Bunge et al. (2002) used a simple box model to illustrate Maul's (1977) theory, applied to data from the Canek observing program (Badan et al., 2005), which deployed eight moorings with acoustic Doppler current profilers and current meters across the YC from 8 September 1999 to 17 June 2000. This 7.5-month record of deep YC transport was compared to the LC area determined from 3-day averaged satellite thermal (Advanced Very High-Resolution Radiometer, AVHRR) images. Bunge et al. (2002) found a very strong relationship between LC area and deep YC flows for this time period. They attributed the lack of a relationship found by Maul et al. (1985) and Maul and Vukovich (1993) to insufficient sampling in the YC. The authors suggested that a longer data set was required to further test and validate Maul's (1977) theory.

To further investigate the results of Bunge et al. (2002), this study uses data from a uniquely long 54-year run of the $1/25^{th}$ degree GoM Hybrid Coordinate Ocean Model (HYCOM; Chassignet et al., 2003; Dukhovskoy et al., 2014). The model is continuously run for three cycles of 18 years, forced with reanalysis atmospheric fields from 1992 to 2009 and forced at the boundaries by climatological fields derived from the $1/12^{th}$ degree North Atlantic HYCOM. This model run provides a long-term data set that is useful to investigate the relationship between changes in LC area and deep YC transport. The multidecadal simu-

lation of the GoM makes it possible to validate Maul's (1977) theory, for the first time to the best of our knowledge. Analysis of the YC deep flow shows a robust relationship with the LC evolution, replicating hypothesized behavior of the system in support of Maul's idea.

Conceptual Model of the GoM Mass Balance

Following Maul (1977), the GoM mass balance can be represented by a simple box model. Assuming incompressibility, mass conservation yields the equation for the rate of change of volume in the GoM,

$$\frac{dV_{GoM}}{dt} = T_Y + T_F + R + (P - E). \quad (1)$$

V_{GoM} is the total volume of the GoM, T_Y is the transport through the YC, T_F is the transport through the FLS (T_F is typically directed out of the GoM and is therefore negative), R is river runoff, P is precipitation, and E is evaporation. Etter (1983) showed that R, P, and E are negligible compared to T_Y and T_F. Also, the rate of change of the GoM volume is negligible compared to the transports through the YC and FLS. This implies that the volume of the GoM is approximately constant. Therefore, the two transport terms, being the two significant terms, approximately balance, i.e.,

$$T_Y + T_F \approx 0. \quad (2)$$

Since the deepest connection to the Atlantic Ocean through the FLS is approximately 730 m (Bunge et al., 2002) and the depth of the YC is approximately 2100 m, it is appropriate to use two layers for the YC (with the upper layer representative of water at

depths that can pass through FLS). Thus, equation (2) becomes

$$T_Y^u + T_Y^l + T_F \approx 0 \qquad (3)$$

where T_Y^u is the transport through the upper YC and T_Y^l is the transport through the lower YC.

Although the GoM volume is constant under the assumptions here, the LC volume varies. The LC is generally confined to the depths of the FLS and of the upper YC, and therefore, the imbalance in mass flux through these openings should govern the rate of change of LC volume. Thus, it can be written

$$\frac{dV_{Loop}}{dt} \approx T_Y^u + T_F. \qquad (4)$$

A caveat associated with this conceptual model is that it does not consider the loss of volume from the LC to the GoM that would occur during the shedding of a LCE. During the period analyzed by Bunge et al. (2002), there were no shedding events. However, during the 54 years of model data used in this study, shedding events do occur. To account for the shedding events, only segments of the deep YC transport and LC area time series between shedding events are analyzed. Other caveats of the model include its assumption of lags between deep YC flow and the LC growth and the difference between the LC depth and the depth of the 6° isotherm in the YC. These additional caveats are discussed further below.

The relation between the LC area and the deep YC transport is readily obtained by combining equations (3) and (4),

$$\frac{dV_{Loop}}{dt} \approx -T_Y^l. \qquad (5)$$

Thus, the rate of change of the LC volume should be approximately equal to the southward deep YC transport, which is the theory presented by Maul (1977) and Bunge et al. (2002).

The schematic in Figure 1 shows the direction of deep YC transport when (a) the LC is growing and (b) the LC is retracting. When the LC is growing, deep YC flow is directed out of the GoM as the LC's deep warm water displaces isopycnals downward. In the schematic, there are two layers divided by a single isopycnal for simplicity. This isopycnal is forced downward when the LC grows, which forces deep water out of the GoM through the YC. The opposite occurs when the LC is retracting.

In previous studies, the deep YC transport was compared to the LC area because the only available observational data of the LC were satellite imagery, and the LC area is assumed to be approximately proportional to its volume. While a three-dimensional hydrodynamic model provides an opportunity to validate this assumption, technical and intellectual challenges related to a three-dimensional tracking of the LC boundaries could have made this effort as a stand-alone study. Indeed, even tracking a two-dimensional contour of the LC at the surface is not

trivial (e.g., Oey et al., 2005; Leben, 2005). Projecting this problem into three dimensions makes this as a major effort that is beyond the scope of this paper. Hence, in this study LC area is also used as a proxy of the LC volume following the work done by Bunge et al. (2002).

Model and Data Description

Data from a 54-year integration of a 1/25° horizontal resolution regional GoM configuration of the HYCOM model (Dukhovskoy et al., 2014) are used to analyze the relationship between the deep YC transport and the LC area. The domain of the model is 18.9°N to 31.6°N and 98°W to 76.4°W (Zamudio & Hogan, 2008) as seen in Figure 2a, which also specifies the cross section of the YC channel used in this study. The model vertical grid consists of 20 hybrid layers. The HYCOM hybrid vertical coordinate system is isopycnal-following in the open, stratified ocean and smoothly reverts to a terrain-following coordinate in the shallow coastal regions and to z-level (geopotential) coordinates in the mixed layer or unstratified seas (Chassignet et al., 2003). The isopycnal

FIGURE 1

A diagram showing deep water leaving the GoM through the YC (on the right side of the diagram) when the LC grows and entering the GoM during LC retraction. This is a two-layer system with the upper and lower layers separated by an isopycnal ρ_1.
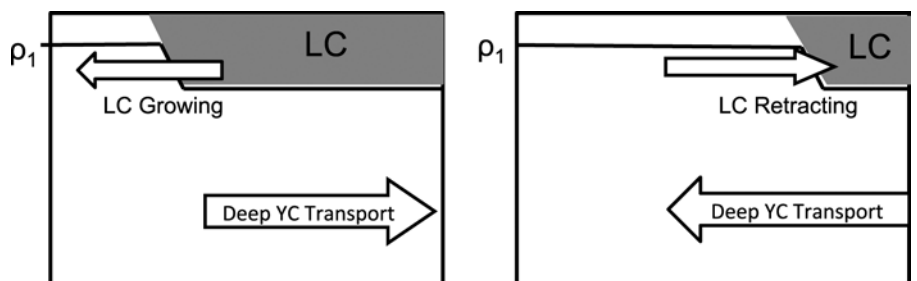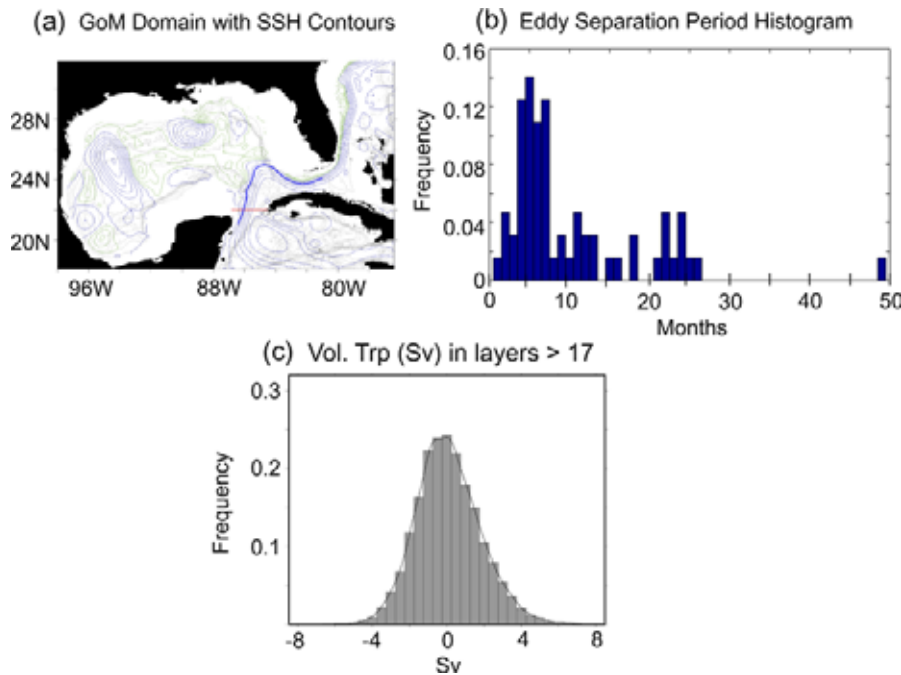
FIGURE 2

(a) The GoM domain with SSH contours; red line indicates location where the transport was calculated in HYCOM. (b) Normalized histogram of the LCE separation period from the 54-year HYCOM simulation. The separation periods on the x-axis are in units of months. (c) Volume transport through the YC in the layers deeper than the 17th layer. The black line is a kernel density estimate that suggests a normal distribution with a mean around zero and a standard deviation of 1.7 Sv. (Color versions of figures are available online at: http://www.ingentaconnect.com/content/mts/mtsj/2014/00000048/00000004.)

(a) GoM Domain with SSH Contours

(b) Eddy Separation Period Histogram

(c) Vol. Trp (Sv) in layers > 17

the GoM deep water where depths exceed 200 m in order to avoid contamination of the areal mean by hurricane forced coastal-trapped waves. The detachment of an LCE from the LC occurs when the 0.17-m LC contour breaks in two separate contours, one is the LC and the other is an LC eddy. Each LC eddy is tracked until it either dissipates or reattaches to the LC. Only events in which eddies detach and ultimately dissipate while separated from the LC are identified as separation events. Satellite sampling limits the smallest LC eddies that can be detected using altimetry, therefore eddies originating from the LC are counted as LC eddy separation events only if their initial areas upon separation are greater than $4,000$ km^2 or about 75 km in diameter. The location of the LC and calculation of its area from the HYCOM simulation follows the algorithm applied by Leben (2005) to gridded satellite altimeter SSH fields. In addition, the reanalysis is performed on a time series with LCE detachment-reattachment events removed through linear interpolation of the LC area time series over the detachment time interval.

The analysis of the timing and frequency of these area drops show that HYCOM realistically portrays LCE shedding events. During the 54 years of daily model SSH fields, the LC sheds 69 eddies. The separation periods, the amount of time between two shedding events, help show the robustness of the model. The model is compared to 18 years of observational data (1993–2010) from altimeter-based SSH gridded fields. This analysis of the observational data yields a mean separation period of 8 months, a median of 6.7 months, and a mode of 6 months. The HYCOM mean separation period is 9.3 months, the

layers are defined by target densities that are chosen such that the layer spacing is reduced (yielding higher vertical resolution) in the upper ocean. The model is forced at the surface with Climate Forecast System Reanalysis (CFSR) atmospheric fields from 1992 to 2009 (Saha et al., 2010). This 18-year subset of CFSR is chosen based on the availability of historical observations for assimilation into the reanalysis. HYCOM is run for three cycles of 18 years, and the ends of the surface forcing time series are blended for a smooth transition between cycles. Since the ocean model simulation is not data assimilative and thus the oceanographic features are not constrained for any given model time, the wind forcing applied in this manner is meant to provide the ocean

model with realistic (rather than real-time) stochastic wind variability.

Boundary conditions for this regional GoM HYCOM are derived from a biweekly climatology of a 4-year 1/12° North Atlantic HYCOM simulation (similar to Zamudio & Hogan, 2008). Even though transports at the boundaries of the GoM HYCOM are prescribed, the test of the box model theory is still valid since the box model represents the interior of the GoM away from the model boundaries.

Following Leben (2005), the LC and LC eddy fronts are tracked using the 0.17-m contour in demeaned SSH fields. Demeaned fields are calculated by subtracting the spatial mean from each daily SSH field. The spatially averaged SSH is calculated over

median is 6.1 months, and the mode is 6 months. Observations have shown a range of separation periods from less than a month to 20 months (Leben, 2005; Vukovich, 2007), whereas HYCOM ranges from 1 to 48 months. The 48-month separation period occurs once, and there are several separation periods over 19 months, indicating that the model occasionally simulates long separation periods that have not been observed (noting that the observational time series is shorter than the model time series). However, the mean, median and mode are reasonable in the simulation. The histogram in Figure 2b illustrates the range of separation periods occurring in the model simulation and their frequency of occurrence.

According to Maul (1977) and Bunge et al. (2002), the LC freely flows from the upper YC to the FLS. Flow that enters the GoM through the deep YC must also exit through the deep YC and therefore the mean flow though the deep YC must be zero, which is seen in the model. To accurately test the box model theory, it is necessary to determine which layers make up the deep YC. These are the vertical layers that have no interaction between the GoM and the Atlantic Ocean through the FLS. It is found that model layer 18 does not connect the GoM to the Atlantic, implying that the 18th layer (representative of water having a density of 1,027.64 kg/m^3) and below make up the deep YC. The average transport through the YC for the 18th layer and below is 0 Sv for the long term (Figure 2c).

YC Flow Structure

Before analyzing the transport time series, it is necessary to determine whether HYCOM portrays the YC

and FLS realistically. Then, to fully understand the mass imbalance and its causes, it is important to understand the variability of the flow structure in the YC and FLS.

The time series of the total HYCOM transports through the YC and FLS (T_Y and T_F) are examined. The two time series are highly related, with a correlation coefficient of 0.98, and they both have a long-term average of approximately 29.5 Sv. This is larger than estimates obtained from the Canek observing program (Sheinbaum et al. 2002), which yielded a mean transport of 23.1 Sv. However, recent observational data from Rousset and Beal (2010) yielded a mean transport of 30.3 Sv over the period of 2001 to 2005. Thus, the mean transport from HYCOM is within the range of recent observational data.

The mean YC flow structure, seen in Figure 3a, from HYCOM is characteristically consistent with observational data from the Canek observing program presented by Sheinbaum et al. (2002). For example, the Yucatan Current, which consists of strong northward flow into the GoM, is mainly located in the upper west portion of the YC. Also, there is consistent southward flow out of the GoM in the upper east portion of the YC. This return flow is the Cuban Countercurrent. The upper YC should be divided into a western portion of northward inflow and an eastern portion of southward return flow. These features vary in time with the size of the LC.

Figure 3b shows the normalized LC area histogram with the 25th and 75th percentiles marked. Figure 3c

FIGURE 3

(a) Cross section of the YC showing the mean flow structure. (b) Normalized LC area histogram with red lines representing the 25th and 75th percentiles. (c) Mean transport (Sv) profiles of the YC when the LC area is larger than its 75th percentile (green) and less than its 25th percentile (red). The mean for the entire simulation is shown in black.
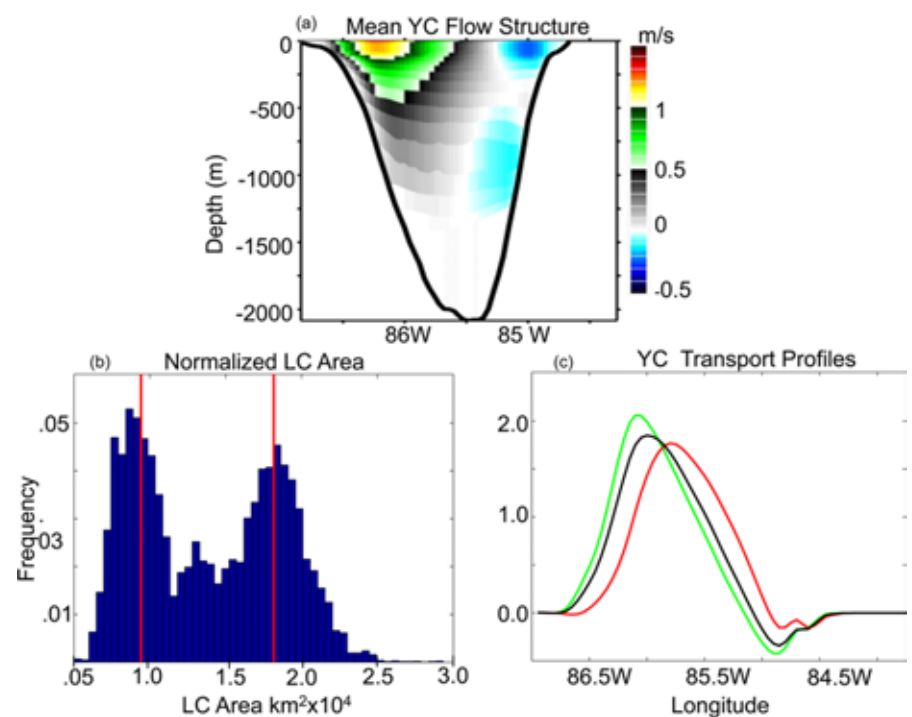
shows the transport profiles of the upper YC (upper 17 vertical layers) for the LC area greater than the 75th percentile and lower than the 25th percentile, as well as the mean transport profile. Here, transport into the GoM is considered positive. When the LC area is below the 25th percentile (red line), the YC current shifts east and broadens, the maximum transport decreases, and the return flow is weak. When the LC area is larger than its 75th percentile (green line), the YC current shifts west, the maximum transport increases, and the return flow out of the GoM increases.

It is useful to think of the upper YC transport in terms of equation (6).

$$T_y^u = T_y^{u+} + T_y^{u-} \qquad (6)$$

T_y^{u+} is the flow into the GoM, mainly to the west, through the upper YC, and T_y^{u-} is the outflow. T_y^{u+} and $-T_y^{u-}$ are well correlated, with a correlation coefficient of 0.73, as suggested by the recirculation.

Thus, mass leaves the GoM through both the YC (T_y^{u-}) and T_f. For the LC to grow, the T_y^{u+} needs to exceed $T_y^{u-} + T_f$. So, even though the Yucatan Current (mainly T_y^{u+}) may be strong, the LC might not be growing if ($T_y^{u-} + T_f$) is also large. The LC should grow only if there is a mass imbalance, according to Maul's (1977) theory. It is noteworthy that in the Maul's conceptual model the recirculation is not explicitly considered. Even though T_y^u consists both of an inflow and a recirculation, T_y^{u+} and T_y^{u-}, the conceptual model still works. T_y^l still balances the difference between the T_y^u and T_f, as seen in equation (7).

$$\left(T_y^{u+} - T_y^{u-}\right) + T_f \approx T_y^l. \qquad (7)$$

Results

To test the hypothesis presented by Maul (1977) and to expand on the results of Bunge et al. (2002), two equations from Bunge et al. (2002) are analyzed. First, after assuming that the LC area is proportional to its volume, equation (5) can be rewritten as

$$H\frac{dA_{Loop}}{dt} \approx -T_y^l \qquad (8)$$

where H is a constant scale depth for the LC and A_{loop} is the LC surface area. The regression linear fit provides a scale depth H of 200 m that yields equality between the left and right side of equation (8). This depth is comparable to the result obtained by Bunge et al. (2002), who found a maximum equivalent depth of the LC of 261 m. This equivalent depth portrays another caveat of the model being that the equivalent depth of the LC is much shallower than that of the 6° isotherm in the YC (Bunge et al., 2002). This balance states that the time rate of change of the LC area should be related to deep YC transport. If the left-hand side of the equation is negative, the LC is retracting. Time series of the LC area consists of high-frequency oscillations superimposed on a positive trend. The trend is associated with a slowly growing LC. Equation (8) describes changes of the LC volume (or area) and the deep YC transport at time intervals Δt, i.e., it represents a high-frequency component of the LC evolution. The low-frequency variability of the LC is obtained by integrating equation (8) over the time interval between two consecutive LCE shedding events:

$$A_{Loop} = A_0 - \frac{1}{H}\int_{t_0}^{t_f} T_y^l(t)dt, \qquad (9)$$

where A_0 is the constant of integration determined from the LC area at the initial time t_0, t_f is the final time, and t is time.

Bunge et al. (2002) showed that both equations (8) and (9) held true for a period of observational data from the Canek observing program. The time range was 7.5 months and included only one case of the LC growth between the eddy separation events. This may not be sufficient to thoroughly test the box model theory. The data from a 54-year run of HYCOM present an opportunity to investigate the theory for a much longer period.

There was no shedding event in the period analyzed by Bunge et al. (2002), and the box model theory does not account for shedding events, as explained previously in Conceptual Model of the GoM Mass Balance. For the theory to hold throughout time and include shedding events, another term would need to be included in the equations to account for extreme losses of volume from the LC (to the LCE) after a shedding event. Instead, to test the box model theory, the LC area time series for HYCOM is segmented into separation periods. A separation period is defined here as beginning the day after a shedding event occurs and ending one day before the next shedding event.

There are 69 shedding events in the HYCOM simulation and therefore 68 separation periods. Each time a segment analyzed begins 30 days after the previous shedding event and ends 30 days before the next shedding event to allow for an adjustment period. For this study, only separation periods of 300 days (the mean separation period) or longer are considered to give a better indication of the validity of the hypothesis since testing the theory over longer periods yields a more robust

result. Short-term shedding events are discarded because, in most cases, they are related to shedding of small LC eddies. From a preliminary analysis, the short-term shedding events do not reveal a robust relationship between the evolution of the LC and deep YC flow. The selection method yields a total of the 22 separation periods.

High-Frequency Variability Comparison

The high-frequency variability between the LC area time derivative and the deep YC transport can be compared using equation (8). Bunge et al. (2002) discovered that filtering with a 20-day running mean revealed a high correlation between the LC area time derivative and deep transports in the YC, suggesting a strong relationship. To compare the results using model data to the Bunge et al. (2002) results derived from observational time series, correlation coefficients are calculated for the terms in equation (8) following application of a 20-day running mean. With the application of the low pass filter, the time series still has high frequencies compared to the time scales of LC variability.

The LC area time derivative with the filter is calculated using equation (10).

$$\frac{dA_{Loop}}{dt(i)} \approx$$
$$1/\Delta t \left(\frac{2}{\Delta i} \left(\sum_{i}^{i+\frac{\Delta i}{2}} \bar{A}_i - \sum_{i-\frac{\Delta i}{2}}^{i} \bar{A}_i \right) \right). \quad (10)$$

This equation applies a centered difference of the 20-day averages before and after a given day i, where Δt is the change in time between the center points of the averaged area $\bar{A}i$ and Δi

is the corresponding number of time steps in days. The variable $\frac{dA_{Loop}}{dt}$ is compared to the 20-day running mean of the deep YC transport from equation (9) and calculated using equation (11).

$$T_y^l(i) \approx \left[\sum_{i-\Delta i/2}^{i+\Delta i/2} T_y^l \right] / \Delta t. \quad (11)$$

After the low pass filter is applied, a relationship becomes evident in HYCOM data (Figures 4a and 4c). Although visual inspection reveals a relationship between the filtered time series, the overall correlation coefficient is 0.39.

Analyzing each separation period individually, we see that for some time periods the correlation is quite strong (>0.50) (Figure 4); however, there are also some segments where the correlation is weak (below 0.1 for three segments). The main reason for the weak correlations is significant variability in the LC area derivative on short time scales, the weakest correlations occurred for segments with the shortest time periods. It is noteworthy that a strong autocorrelation in the time series complicates the calculation of significance of the correlation (Chatfield, 1996). Nevertheless, the correlation coefficients are used here to measure the tendency of coherence between the time series and to compare with the results of Bunge et al. (2002). A different approach to verifying the relationship between deep YC transport and the LC area (volume) in which significance of the relation may be evaluated is presented below in Low-Frequency Variability Comparison using a linear regression approach.

FIGURE 4

The scale depth H multiplied by the LC area time derivative (blue) and deep YC transport (red) for three separation periods. The correlations and temporal lengths are (a) 0.50, 671 days; (b) 0.50, 829 days; and (c) 0.59, 605 days.
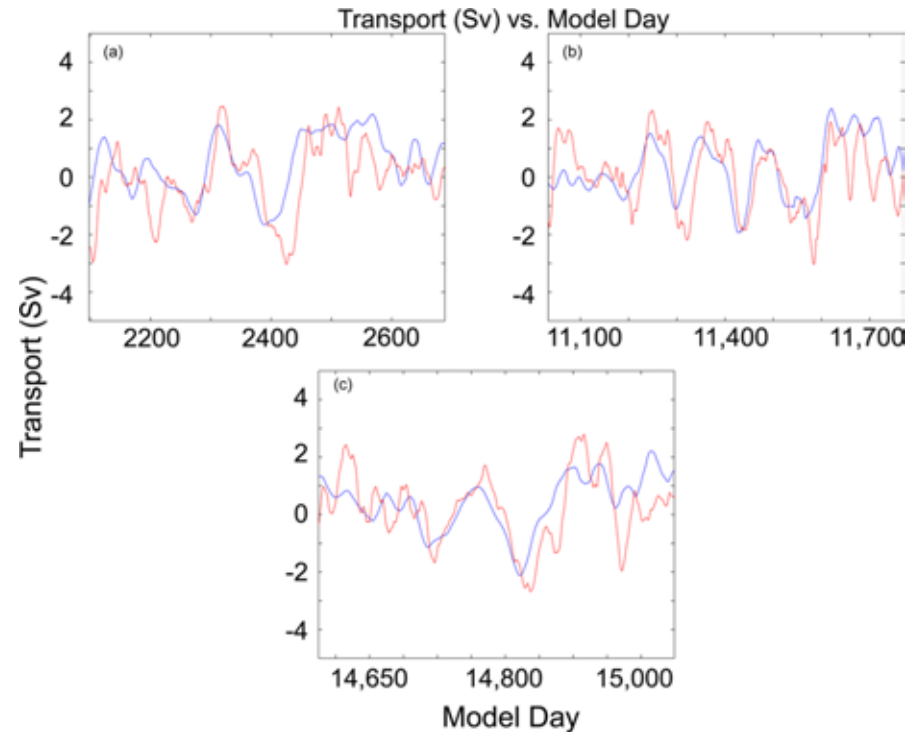
The correlation is also impacted by an apparent lag in several of the separation periods—the deep YC transport lags the LC area time derivative. This is very noticeable in Figure 4. Bunge et al. (2002) found that, for their data, the correlation between the LC area time derivative and the deep YC transport increased from 0.62 with no lag to 0.83 when the deep YC transport lagged the LC area time derivative by 8.6 days. This was noted as suggestive of an internal adjustment period for the GoM, attributable to the first baroclinic mode of a Kelvin wave. They stated that the first baroclinic mode of a Kelvin wave would take approximately 8 days to travel around the GoM, which is close to this lag time.

For the 22 combined separation periods in HYCOM, the correlation is maximized when a lag of 11 days is applied. This lag increases the overall correlation from 0.39 to 0.47. This increase seems far less significant than that found by Bunge et al. (2002) when a lag is applied. This smaller increase is because of the length of the HYCOM series compared to the data from the Canek observing program. The length of the time series and the differences between the separation periods themselves make it reasonable to apply individual lags to each separation period, thereby providing a distribution of lags, which implies a range of plausible lags.

The majority of the separation periods in the HYCOM simulation have a maximum correlation for lags ranging from 9 to 16 days, with 9 days being the most common lag. There are a couple of outliers that yield best lags over 20 days. However, the most frequent best lag, 9 days, is reasonably similar to that found in Bunge et al. (2002), and it is consistent with an

Scatterplot of the product of LC area time derivative and a scale depth (200 m) versus the transport averaged over the same time frame ($\Delta t = 20$ days). The transport is negated here to show a positive slope. The slope is 0.9389 with an uncertainty of 0.1166. The LC area is multiplied by a scale depth H for equivalent units.
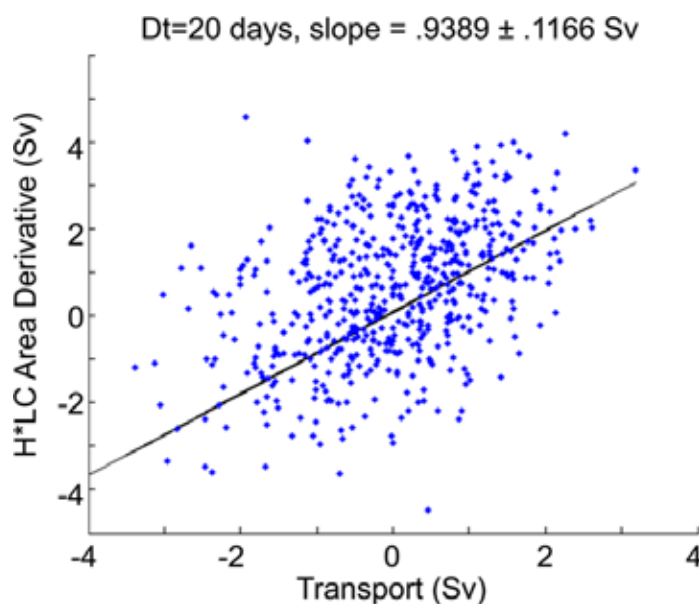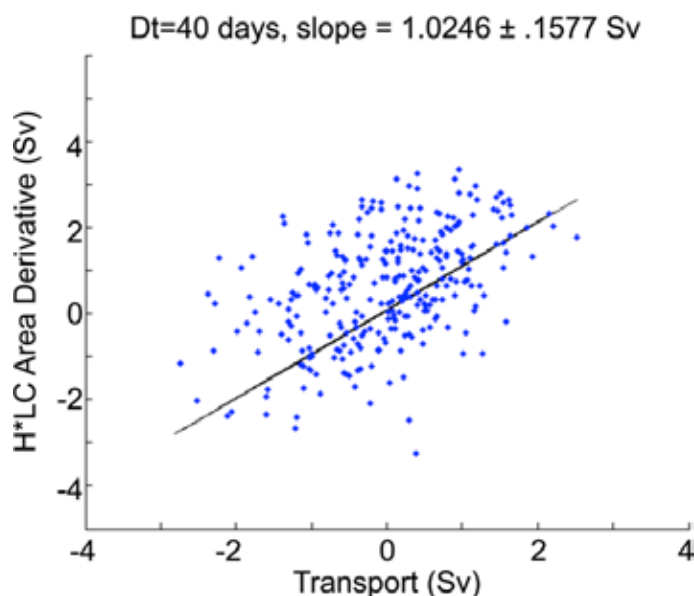
Scatterplot of the LC area time derivative versus the transport averaged for $\Delta t = 40$ in equation (10). The slope is 1.0246 with an uncertainty of 0.1577. The LC area is multiplied by a constant depth H for equivalent units.

adjustment period related to the first baroclinic mode of a Kelvin wave.

If the two series are filtered for more than the 20 days chosen by Bunge et al. (2002), the correlation further increases. A spectral analysis shows a peak in the variability of the deep YC transport around 40 days, and thus, a 40-day filter is applied. Bunge et al. (2002) also noted that in their data set there was a dominant mode of variability around 40 days.

The correlation coefficient for the overall time series is 0.58 when the 40-day filter is used. Therefore, over a third of the total variance is explained. The increase in the correlation is largely due to the decrease in variability of the transport time series. When the 1l-day lag is applied to the time series with the 40-day running mean, the correlation increases from 0.58 to 0.65 and the maximum correlation for an individual separation period is 0.89.

The relationship between changes in the LC area and the deep YC transport is further analyzed using a linear regression and is viewed easily with a scatterplot. Each point on the scatterplot shows the LC area time derivative for a given deep YC transport. The LC area time derivative for the scatterplot is calculated using equation (12).

$$\frac{dA_{Loop}}{dt} = \frac{A_{Loop_{i+\Delta i}} - A_{Loop_i}}{\Delta t} \qquad (12)$$

Here, i represents a day in the time series, Δt is the amount of time between two points for which a difference is being calculated, and Δi is the corresponding change in time steps. Thus, equation (12) effectively yields a forward difference over the length of time, Δt. Over the same Δt, the deep YC transport is approximated by the average transport.

The scatterplot for $\Delta t = 20$ days without reattachments shown in Figure 5 suggests a linear relationship between the two with the slope of 0.9389 (± 0.1166). The scatterplot is effectively showing that the larger the change in LC area, the stronger the negative deep YC transport. This relationship supports the theory presented by Maul (1977) and elaborated by Bunge et al. (2002).

The time series of the deep YC transport is found to have a peak in variability around 40 days. Therefore, a scatterplot using a 40-day time difference ($\Delta t = 40$ in equation (12)) is created. The slope for the 40-day scatterplot, shown in Figure 6, is 1.0246 (± 0.1577). This slope shows indicates a relationship between deep YC transport LC area.

The relationship between the LC area time derivative and the deep YC transport is summarized with histograms (Figure 7). From equation (8), it follows that, when the LC area time derivative is positive, the YC deep flow is out of the GoM, and vice versa, when the LC area time derivative is negative (LC slowly retreats), the YC deep flow is into the GoM. The histograms in Figure 7 display the frequency at which negated deep transports ($-T_y^l$) occur when the LC area time derivative is greater than its 75th percentile (5,500 m^2/s), and when the LC area time derivative is less than its 25th percentile (–1000 m^2/s) for the combined 22 segments. It is clear that, for the 75th percentile and above (top panel in Figure 7), $-T_y^l$ is usually positive, that is, the YC deep flow is directed out of the GoM. The negative changes in the LC area (bottom panel in Figure 7) are almost always negative ($-T_y^l < 0$) indicating inflowing deep water into the GoM through the YC. There is a very clear separation showing that the theory proposed by Maul (1977) is supported in HYCOM.

Low-Frequency Variability Comparison

The time series of the LC area is compared to the time integration of the deep YC transport (equation (9))

Probability density functions showing the probability of negated deep YC transports ($-T_y^l$) occurring when the LC area is (a) greater than its 75th percentile and (b) less than its 25th percentile.
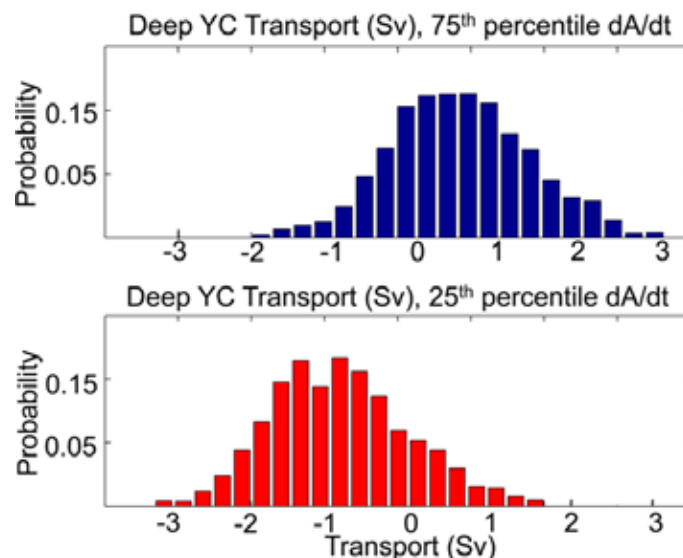
to examine the relationship between the two time series at low frequencies (comparable to the eddy shedding frequency). It is anticipated that, when the LC area increases, the time integration of the deep transport over the same period should increase at a similar rate. As an illustration, three separation periods are shown in Figure 8 where matching linear regressions are easily seen. The consistency of the slopes between the time integrated deep YC transport and LC area supports the validity of the conceptual model.
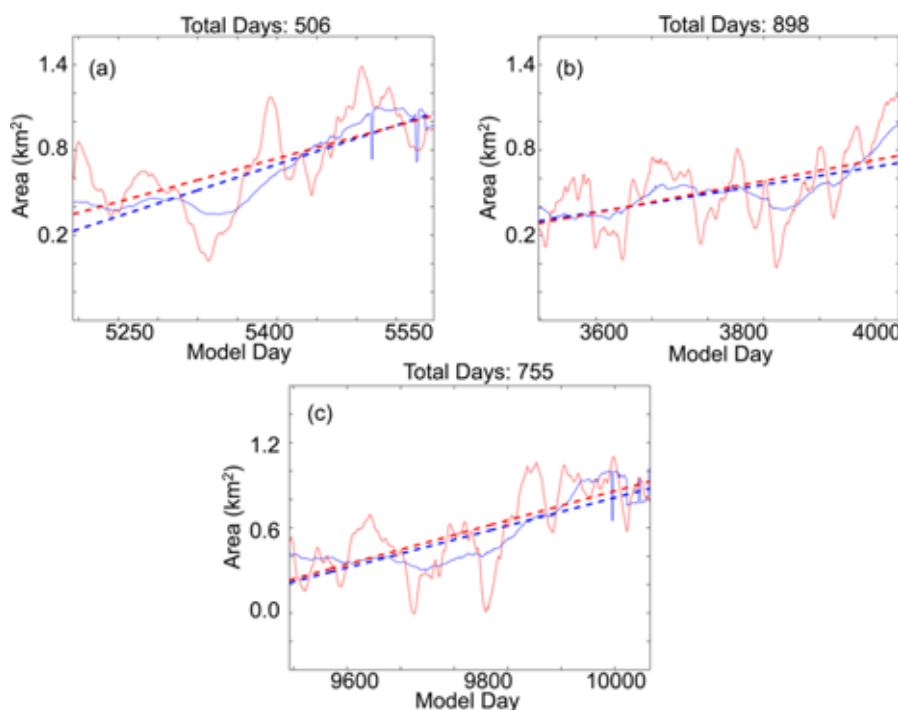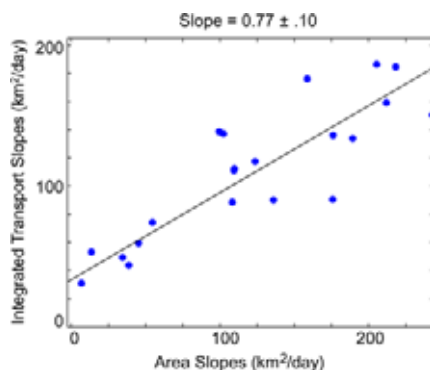
An analysis of each segment's slope from the linear regression yields the statistical significance of the relationship between the LC area and the time-integrated transport. It is found that the linear regressions of the time series are quite similar for each separa-

tion period as seen in the scatter plot (Figure 9). This scatter plot shows that the linear regressions' slopes for each segment are quite similar. This is a robust result considering the

variation of slopes from segment to segment. The mean slope for the time integrated deep YC transport is 105 km^2/day and 113 km^2/day for the LC area. A t-test shows the means to be statistically equivalent, meaning that it is highly likely that these two time series are related.

Conclusion

Data from a 54-year run of the 1/25th degree GoM HYCOM model are used to analyze a theory, first proposed by Maul (1977), that changes in LC volume in time should be compensated for by deep flows in the YC.

The box model theory is tested with HYCOM after the deep YC is defined as the 18th isopycnal (target density of 1,027.64 kg/m^3) and below. To accurately test the box model theory, it is necessary to use segments between eddy shedding events. Of the 69 available separation periods, 22 are used. The selection criterion is that the separation period has to be at least 300 days (the mean separation period) or longer.

A conceptual model of the GoM mass budget is tested using the 54-year simulation. The first equation tested, equation (8), is used to compare the high-frequency relationship between the LC area and deep YC transport. After a 20-day running mean for each time series is applied, a relationship between the two time series becomes evident. Though the correlations are fairly weak (for the combined 22 separation periods, it is only 0.39), it is clear that, when the LC is growing, more mass is leaving the GoM through the deep YC and hence there is an imbalance between the upper YC transport and the FLS. Applying a 40-day running mean improves the relationship between the LC area and

deep YC transport. The correlation analysis suggests that the deep YC flow lags the LC area change. The lags range from 9 to 16 days, which is similar to the 8.6-day lag found in Bunge et al. (2002).

Scatterplots and histograms illustrate the relationship between the growth of the LC and the deep YC transport. Both the 20-day and 40-day scatterplots show the negated deep YC transport increasing as the LC area growth rate increases. The linear regression shown by the scatterplot illustrates the statistical significance of the relationship.

The relationship between the LC area and the time integration of the deep YC transport (equation (9)) are tested and used to compare the low-frequency variations in the data. For the 22 separation periods analyzed, the regression analysis indicates relationship between the LC area and the time integration of the deep YC transport in HYCOM that is statistically significant. The low-frequency comparison between the LC area and the deep YC transport further supports that variability in the deep YC transport is related to variability in the LC growth.

In conclusion, the theory proposed by Maul (1977) and supported by an analysis of a somewhat short (compared to the LC eddy shedding cycle) observational data set by Bunge et al. (2002) is further supported by analysis of a high-resolution multidecadal free-running model that realistically simulates the LC and eddy behavior. Though a longer observational record would be required to conclusively verify the theory, this work has yielded additional confidence that there is a significant relationship between the transport through the deep YC and the evolution of the LC.

Acknowledgments

Corresponding Author:

Robert Nedbor-Gross
Center for Ocean-Atmospheric Prediction Studies,
The Florida State University,
Tallahassee, FL
Email: rnedbor1@ufl.edu

References

Badan, A., Candela, J., Sheinbaum, J., & Ochoa J. 2005. Upper-layer circulation in the approaches to Yucatan Channel. In: Circulation in the Gulf of Mexico: Observations and Models, eds. Lugo-Fernandez, A. & Sturges, W., pp. 57-69. Washington, DC: AGU.

Bunge, L., Ochoa, J., Badan, A., Candela, J., & Sheinbaum, J. 2002. Deep flows in the Yucatan Channel and their relation to changes in the Loop Current extension. J Geophys Res. 107(C12):3233. doi: 10.1029/2001JC001256.

Chassignet, E.P., Smith, L.T., Halliwell, G.R., & Bleck, R. 2003. North Atlantic simulation with the Hybrid Coordinate Ocean Model (HYCOM): Impact of the vertical coordinate choice, reference density, and thermobaricity. J Phys Oceanogr. 33:2504-26. http://dx.doi.org/10.1175/1520-0485(2003)033<2504:NASWTH>2.0.CO;2.

Chatfield, C. 1996. The Analysis of Time Series: An Introduction. London: Chapman & Hall. 283 pp.

Dukhovskoy, D.S., Chassignet, E.P., Hall, C., Leben, R.R., Morey, S.L., & Nedbor-Gross, R. 2014. Characterization of the Uncertainty of Loop Current Metrics Using a Multidecadal Numerical Simulation and Altimeter Observations. Manuscript, under review.

Dukhovskoy, D.S., Morey, S.L., Martin, P.J., O'Brien, J.J., & Cooper, C. 2009. Application of a vanishing, quasi-sigma, vertical coordinate for simulation of high-speed, deep currents over the Sigsbee Escarpment in the Gulf of Mexico. Ocean Model. 28(4):250-65. http://dx.doi.org/10.1016/j.ocemod.2009.02.009.

Etter, P.C. 1983. Heat and freshwater budgets of the Gulf of Mexico. J Phys Oceanogr. 13:2058-69. http://dx.doi.org/10.1175/1520-0485(1983)013<2058:HAFBOT>2.0.CO;2.

Gierach, M.M., Subramanyam, B., & Thoppil, P.G. 2009. Phyiscal and biological responses to Hurricane Katrina (2005) in a 1/25° nested Gulf of Mexico HYCOM. J Mar Sys. 78:168-79. doi: 10.1016/j.jmarsys.2009.05.002.

Hurlburt, H.E., & Thompson, J.D. 1980. A numerical study of Loop Current intrusions and eddy shedding. J Phys Oceanogr. 10:1611-51. http://dx.doi.org/10.1175/1520-0485(1980)010<1611:ANSOLC>2.0.CO;2.

Leben, R.R. 2005. Altimeter-Derived Loop Current Metrics. In: Circulation in the Gulf of Mexico: Observations and Models, eds. Sturges, W., & Lugo-Fernandez, A. Washington, DC: AGU. doi: 10.1029/161GM15.

Lugo-Fernandez, A. 2007. Is the loop current a chaotic oscillator? J Phys Oceanogr. 37:1455-69. http://dx.doi.org/10.1175/JPO3066.1.

Maul, G.A. 1977. The annual cycle of the Gulf Loop Current, part I, Observations during a one-year time series. J Mar Res. 35:29-47.

Maul, G.A., Mayer, D.A., & Baig, S.R. 1985. Comparison between a continuous three-year current meter observation at the sill of the Yucatan Strait, satellite measurements of Gulf Loop Current area, and regional sea level. J Geophys Res. 90:9089-96. http://dx.doi.org/10.1029/JC090iC05p09089.

Maul, G.A., & Vukovich, F.M. 1993. The relationship between variations in the Gulf of Mexico Loop Current and the Straits of Florida volume transport. J Phys Oceanogr. 23:785-96. http://dx.doi.org/10.1175/1520-0485(1993)023<0785:TRBVIT>2.0.CO;2.

Morey, S.L., & Dukhovskoy, D.S. 2013. A downscaling method for simulating deep current interactions with topography–application to the Sigsbee Escarpment. Ocean Model. 69:50-63. http://dx.doi.org/10.1016/j.ocemod.2013.05.008.

Oey, L.-Y., Ezer, T., Forristall, G., Cooper, C., DiMarco, S., & Fan, S. 2005. An exercise in forecasting loop current and eddy frontal positions in the Gulf of Mexico. GRL. 32:L12611. doi:10.1029/2005GL023253.

Rousset, C., & Beal, L.M. 2010. Observations of the Florida and Yucatan Currents from a Caribbean Cruise Ship. J Phys Oceanogr. 40:1575-81. doi: 10.1175/2010JPO4447.1.

Saha, S., & Coauthors 2010. The NCEP climate forecast system reanalysis. Bull Amer Meteor Soc. 91:1015-57. doi: 10.1175/2010BAMS3001.1.

Sheinbaum, J., Candela, J., Badan, A., & Ochoa, J. 2002. Flow structure and transport in the Yucatan Channel. Geophys Res Lett. 29(3):1040. doi:10.1029/2001GL013990.

Sturges, W. 1994. The frequency of ring separation from the loop current in the Gulf of Mexico. J Mar Res. 41:639-53. http://dx.doi.org/10.1357/0022240083788520487.

Vukovich, F.M.. 2007. Climatology of ocean features in the Gulf of Mexico using satellite remote sensing data. J Phys Oceangr. 37:689-707. doi: 10.1175/JPO2989.1.

Zamudio, L., Hogan, P.J. 2008. Nesting the Gulf of Mexico in Atlantic HYCOM: Oceanographic processes generated by Hurricane Ivan. Ocean Model. 21:106-25. http://dx.doi.org/10.1016/j.ocemod.2007.12.002.